Laser-driven anisotropic and nonlinear Rashba spin splitting in GaAs monolayer

Lei Sun,[1] Xikui Ma,[1] Jian Liu,[1,*] and Mingwen Zhao[1,2,†]
[1]*School of Physics, Shandong University, Jinan, Shandong, 250100, China*
[2]*State Key Laboratory of Crystal Materials, Shandong University, Jinan, Shandong, 250100, China*

(Received 24 March 2021; revised 1 August 2021; accepted 4 August 2021; published 23 August 2021)

We investigate the electronic properties of the buckled honeycomb GaAs monolayer under a periodically circularly polarized laser (CPL) by first-principles calculations and Floquet theory. Under the irradiation of CPL with propagation direction in the *xy* plane, a remarkable Rashba spin splitting (RSS) is induced in the valence and conduction bands at Γ point. The laser-driven RSS deviates from the classical linear Rashba model in a wide range of wave vectors, and can be interpreted by a nonlinear model involving the third-order terms. The phase diagram of Rashba effect with laser amplitude and propagation direction is worked out. The anisotropy of the nonlinear RSS is mainly determined by the laser propagation direction, providing the possibility of controlling the Rashba anisotropy characteristics. By carefully choosing the laser frequency and amplitude, giant anisotropic RSS can be obtained, which allows the generation of spin-polarized electrons via doping and facilitates the flexibility of spintronic devices.

DOI: 10.1103/PhysRevB.104.085140

I. INTRODUCTION

Motived by the great successes of graphene [1], two-dimensional (2D) materials have aroused great interest, due to the distinct properties and fascinating physical scenarios arising from the unique lattice structures and quantum confinement effect. The exotic electronic structures and the related properties, such as the quantum spin Hall effect and the quantum anomalous Hall effect, hold great promises in the next-generation devices. A huge number of 2D materials have been proposed theoretically and synthesized experimentally, offering a solid basis for the investigation and utilization of 2D materials. Among them, the 2D materials with a honeycomb lattice, in analog to graphene have been intensively studied, uncovering many interesting properties, such as topological insulators [2,3], electronic spin polarization, and valley splitting [4–6].

Single-layer group-III-V binary compounds have the advantages of natural band gap and the valley or Rashba splitting due to the absence of inversion symmetry [7,8]. Except for BN that has a planer configuration, many binary compounds prefer a buckled geometry, which can be attributed to the destabilization of the π bonds of sp^2-hybridized atoms and the increase of bond length [9,10]. For example, the GaAs monolayer exhibits a buckled honeycomb geometry [10–13]. First-principles calculations show that the GaAs monolayer is an intrinsic indirect band gap semiconductor, and can be tuned to a direct band gap semiconductor or even a metal by hydrogenation or applying electric field [14,15].

Spin-orbit coupling (SOC) originates as one of the relativistic effects of electrons and can lift the spin degeneracy of the electronic states in the materials without inversion symmetry, which is known as the Rashba spin splitting (RSS) [16,17]. This offers a promising strategy to achieve extraordinary topological properties in superconducting and cold atom systems, e.g., bosonic topological states stabilized by interactions [18], which has brought an abundance of research in the electronic devices. It has been demonstrated that RSS can be regulated by electric field or external strain [19–22]. However, the integration of electric field or external strain increases the complexity of devices. Developing a noncontacting and reversible approach to tune RSS of 2D materials is desirable.

Laser has been employed to modulate the electronic properties of materials [23–29]. Under the periodic laser driven field, the electronic structure is dressed by the virtual photon process. Sidebands are formed as the replicas of the original bands by multiples of photon energy [30–34]. Such a system would be driven into a nonequilibrium state due to the continuous time translational invariance breaking, which is named the Floquet-Bloch band [35–38]. Some interesting scenarios, such as Floquet-Weyl semimetals [39–44], quantum anomalous Hall state [45,46], and Majorana Fermions [47–49], have been demonstrated in the laser-modulated materials. The laser modulation technique has the advantages of easy operation without the need of complicated device structures and thus is drawing increasing interest.

Here, using first-principles calculations, we investigate the RSS of the GaAs monolayer modulated by periodic circularly polarized laser. It is found that the laser-induced RSS in the GaAs monolayer exhibits anisotropic and nonlinear features, as shown in Fig. 1. The anisotropy in weak laser intensity is correlated to the propagation direction of circularly polarized laser, while the nonlinear characteristics can be interpreted by using an effective Rashba Hamiltonian involving a third-order term. By carefully choosing the laser frequency and amplitude, giant anisotropic RSS can be obtained, which holds great promise in spintronic devices.

*liujian2019phd@gmail.com
†zmw@sdu.edu.cn

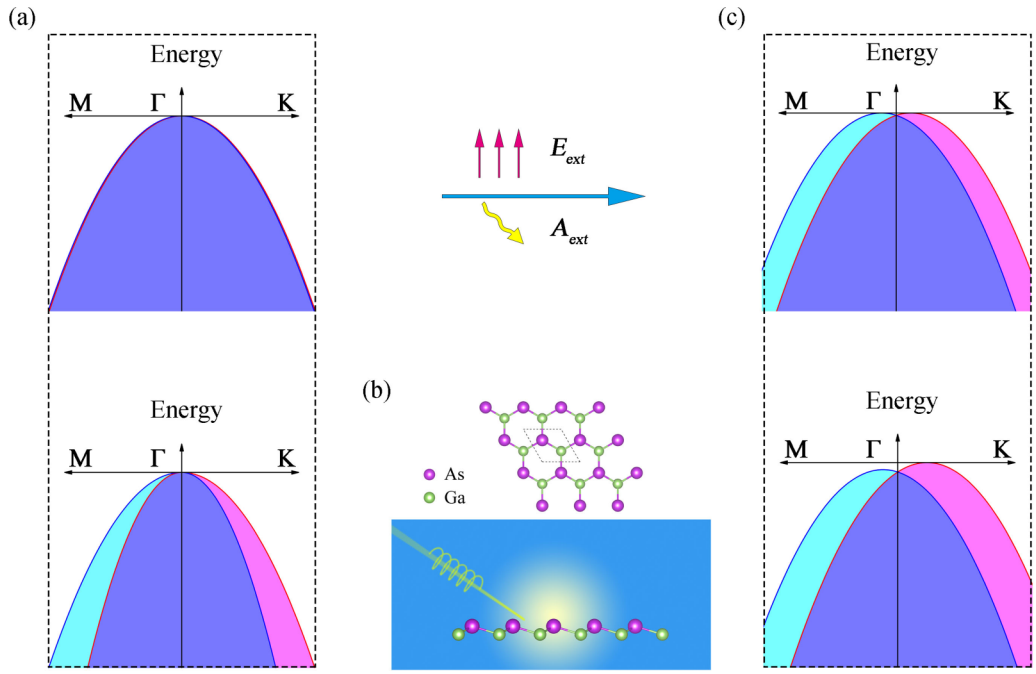

FIG. 1. Schematic view of RSS with spin-orbit coupling effect induced by electric or laser fields. (a) no RSS of two bands with equal (upper panel) and different (lower panel) effective masses. (b) Schematic of structure and laser induction operation of the GaAs monolayer. (c) Isotropic (upper panel) and anisotropic (lower panel) RSS.

II. METHODS

The structure optimization and electronic structure calculation of the GaAs monolayer were performed using the plane wave basis Vienna *ab initio* simulation package known as the VASP code implementing the density functional theory (DFT) [50,51]. The electron exchange-correlation functional was treated using a generalized gradient approximation in the form proposed by Perdew, Burke, and Ernzerhof [52]. The electron-ion interaction was described by projector-augmented-wave potentials [53]. The energy cutoff of the plane-wave basis was 500 eV. The atomic positions and lattice vectors were fully optimized using the conjugate gradient scheme until the maximum force on each atom was less than 0.01 eV/Å. For the 2D structures, the Brillouin zone was sampled by using a 19 × 19 × 1 Gamma-centered Monkhorst-Pack grid. The vacuum space was set to at least 20 Å along the out-of-plane direction to minimize artificial interactions between neighboring slabs. SOC was included by a second-variational procedure on a fully self-consistent basis.

The Hamiltonian of Floquet calculations was obtained on the basis of the maximum localized Wannier functions [54]. The effect of the periodic laser field was treated via Peierls substitution. In our calculation, the limitation of two photon processes is adopted for all results to reduce unnecessary computation, i.e., the matrix is truncated at fifth order ($n = -2, -1, 0, 1, 2$). The details for the Floquet analysis are presented in the Supplemental Material (SM) [55,56].

III. RESULTS AND DISCUSSION

The GaAs monolayer has a buckled honeycomb lattice in space group of P3m1 (No. 156, its point group at Γ point is C_{3v}) with the altitude of 0.594 Å measured from the distance between the two atomic planes. The optimized lattice constant (the length of basis vectors) is 4.056 Å, which is consistent with the data of previous works [7,15]. Each Ga atom is connected to three nearest As atoms and vice versa with a bond length of 2.416 Å. The stability of the GaAs monolayer has been verified from first-principles calculations [7,15]. The recent progress on the synthesis of AlN multilayers [57,58] may shed light on the realization of the GaAs monolayer.

Figures 2(a) and 2(b) shows the electronic band structure of the GaAs monolayer without and with SOC. We can see that the GaAs monolayer is an indirect bandgap semiconductor with the conduction band minimum (CBM) and the valence band maximum (VBM) residing at the Γ and K points, respectively. The SOC in this noncentrosymmetrical monolayer gives rise to a small RSS in the conduction band, but the spin degeneracy of the valence bands at the Γ point is preserved (see the SM for a zoom-in view).

Then we introduce a time-dependent irradiation of laser $\boldsymbol{A}(\tau) = A_0[\cos(\omega\tau)\mathbf{x} + \eta\sin(\omega\tau)\mathbf{z}]$, where ω is the frequency and A_0 is the amplitude of the laser, $\eta = \pm 1$ represents the chirality of the circularly polarized laser. In our calculations, the frequency is set to be comparable to the bandwidth, which is also attainable in pump-probe experiments. The band structures of the GaAs monolayer in the laser field are obtained by using the Floquet theory in combination with a tight-binding Hamiltonian parametrized from first-principles calculations. With the increase of laser amplitude, the band structures show the following features as shown in Figs. 2(a)-2(e): (i) the RSS of the conduction band is enlarged, while a small RSS emerges in the valence band at the Γ point; (ii) the "VBM" gradually shifts from the K point to the Γ point, leading to an indirect-to-direct-bandgap transition; (iii) both the energy

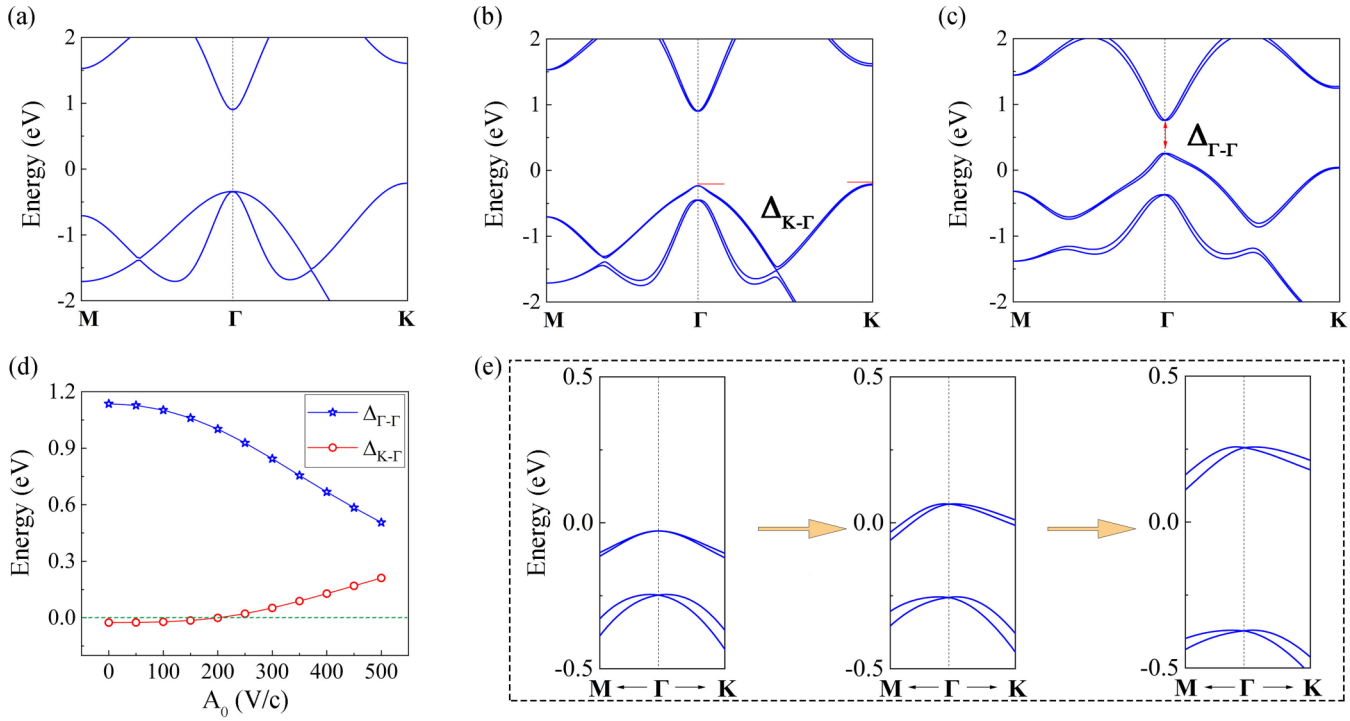

FIG. 2. Electronic band structures of the GaAs monolayer (a) without SOC, (b) with SOC and (c) under a laser field with a frequency of 4.5 eV and $A_0 = 500$ V/c. (d) The variation of the band gaps as a function of laser amplitude. (e) The enlarged diagram of the RSS of the valence bands as the laser amplitude varies from 100, to 300 and 500 V/c. The energy of the Fermi level is set to that of the ground state.

of CBM and the overall band gap decreases. To illustrate the latter two points clearly, we define $\Delta_{K-\Gamma} = E_\Gamma^{VB} - E_K^{VB}$ and $\Delta_{\Gamma-\Gamma} = E_\Gamma^{CB} - E_\Gamma^{VB}$, which represent the energy difference of the valence band between the K and the Γ point, and the energy difference between the conduction band and valence band at the Γ point, respectively, as shown in Fig. 2(b) and 2(c). The relationship of these two quantities with the laser amplitude is plotted in Fig. 2(d). The "location handover" of the "VBM" takes place at $A_0 \sim 200$ V/c. Figure 2(e) shows the band structures with SOC in the region near the Γ point under a 4.5 eV driving field with $A_0 = 100$, 300, and 500 V/c, respectively (see the SM for the case of conduction band).

To describe the laser-induced RSS (Δ_{RSS}) of the two valence bands, we define

$$\Delta_{\mathrm{RSS}} = \sqrt{|\Delta E_F(\boldsymbol{k})|^2 - |\Delta E_O(\boldsymbol{k})|^2}, \tag{1}$$

where ΔE_F and ΔE_O are, respectively, the energy splitting with and without laser (see SM for details). The variation of Δ_{RSS} as a function of k along the Γ-M and Γ-K directions under a 4.5 eV driving frequency with $A_0 = 250$ V/c is plotted in Fig. 3(a). It is found that in the range of relatively small momentum region (0.015 Å^{-1}), the linear terms α_1^M and α_1^K are dominating, exhibiting linear characteristics with $\alpha_1^M = 0.403$ eV Å and $\alpha_1^K = 0.252$ eV Å. Unlike the case of large electric-field-induced RSS [59,60], the laser-induced linear RSS appears in a relatively narrow momentum space. The linear and nonlinear coefficients as a function of laser amplitude are displayed in Fig. 3(b). With the increase of laser amplitude, the linear RSS coefficients (α_1^K and α_1^M) are almost linearly dependent on the laser amplitude. Meantime, it is obvious that the coefficient along the Γ-M direction is much larger than that along the Γ-K direction. Such a difference is more obvious in Fig. 2(e) which can be correlated to the laser propagation direction.

In contrast to the case of the valence band, the conduction band exhibits intrinsic RSS in the absence of illumination with isotropic and linear relation to the momentum, as shown in Fig. 3(c). The laser field enhances the RSS, resulting in nonlinear relation with momentum. Notably, the RSS of the CB is about four times larger than that of the VB, indicating the strong Rashba effect of the conduction band.

In the 2D electron gas model, the effective Hamiltonian of Rashba terms can be expressed as

$$H_R(\boldsymbol{k}) = \alpha_R(k_x\sigma_y - k_y\sigma_x), \tag{2}$$

where $\alpha_R = \frac{\hbar^2}{4m^2c^2}\int d^3r|\phi(z)|^2\partial_z V(\boldsymbol{r})$ is the Rashba parameter and $\sigma_i (i = x, y, z)$ represent the Pauli matrices. The corresponding energy eigenvalues, $\varepsilon_\pm(\boldsymbol{k}) = \varepsilon_0 + \frac{\hbar^2\boldsymbol{k}^2}{2m^*} \pm \alpha_R|\boldsymbol{k}|$, contain an isotropic Rashba SOC term which is linearly dependent on k. The validity of this isotropic linear Rashba term has been verified in many systems [16,17,19–22]. For the anisotropic cases, such as the surface states of Au (110) surface [59,61–63] with a C_{2v} symmetry, an anisotropic Rashba Hamiltonian term is involved beside the asymmetry of the effective mass, which contains two independent Rashba parameters (α_R^1, α_R^2):

$$H_R(\boldsymbol{k}) = \alpha_R^1 k_x\sigma_y + \alpha_R^2 k_y\sigma_x. \tag{3}$$

Despite the successes of the linear Rashba model in many systems, there are still reports that the RSS in certain semiconductor quantum wells deviates from the linear behavior [64–67]. The nonlinear RSS offers a platform for

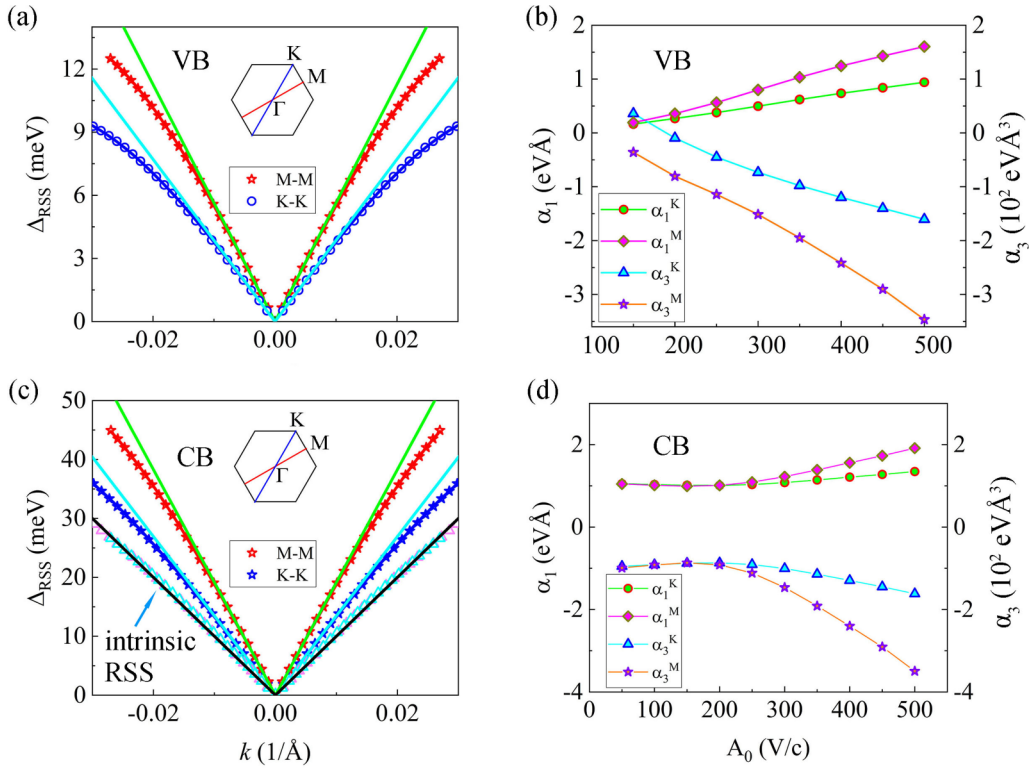

FIG. 3. The relation between the Δ_{RSS} and the wave vector k along the Γ-M and Γ-K directions under laser field with a frequency of 4.5 eV and amplitude of $A_0 = 250$ V/c for valence band (a) or $A_0 = 500$ V/c for conduction band (c). The cyan and pink triangles in (c) represent the intrinsic RSS. The dots are directly calculated by DFT, and the curves with same color as the dots represent the fitting results from the Rashba Hamiltonian. The tangent lines of the dots are obtained by only considering the linear terms in the Rashba Hamiltonian. (b), (d) The amplitude dependence of the linear coefficient α_1 and nonlinear coefficient α_3 along the Γ-M and Γ-K directions.

both underlying physics and device application. For the GaAs monolayer, the combined effect of SOC and laser field leads to remarkable anisotropy of the band structure, i.e., the Rashba-like band lines and the valence bands with different effective masses. We thus adopted an anisotropic Hamiltonian which contains nonlinear Rashba term [59] to describe the RSS of the valence and conduction bands:

$$H_R = \left(\alpha_1 k_x + \alpha_3 k_x^3\right)\sigma_y + \left(\alpha_1' k_y + \alpha_3' k_y^3\right)\sigma_x, \qquad (4)$$

where α_1, α_3, α_1' α_3' represent the linear and cubic coefficient in the k_x and k_y direction which can be obtained by fitting the data of first-principles calculations. Notably, the laser induced strong anisotropy along the two different directions is nearly independent. Thus, the parameters setting here is different from Ref. [60].

In addition, we notice that the nonlinear coefficient of VB along the Γ-K direction changes from positive to negative in Fig. 3(b), meaning that the RSS is linear at a certain laser amplitude (∼150 V/c). Thereby, we define the region of $|\alpha_3^K| \leqslant 30$ eV Å^3 as "linear region" since the energy difference needed to be compensated is relatively small. Based on the above definition, the phase diagram of "linear regions" in frequency-amplitude space is displayed in Fig. 4(a). It can be seen that the "linear region" is concentrated in a narrow amplitude range and is almost independent of the laser frequency. In the nonlinear region, increasing the laser amplitude will enlarge the nonlinear RSS coefficient; For the same laser amplitude, the large nonlinear effect appears more likely in the low-frequency range, which is related to the enhanced interaction between the original bands and dressed side bands. For the RSS of CB, there is no linear region under the same definition, which can also be seen from Fig. 3(d). The nonlinear phase diagrams along another direction (Γ-M) of the CB and VB are shown in Fig. S5, with no linear region obtained either.

Moreover, the anisotropy of RSS can also be tuned by controlling the direction of laser propagation. To reveal the origins of the scenario that the anisotropy of laser-induced Rashba is related to laser propagation direction, we consider the case of the circularly polarized laser with a vector potential $A_0(\cos\theta\cos\omega\tau,\ \sin\theta\cos\omega\tau,\ \gamma\sin\omega\tau)$ and calculate the corresponding RSS values. The laser propagation direction is in the xy plane and varies with an angle of θ relative to the x axis. The relevant phase diagram of the anisotropic parameter defined as $\eta = (\alpha_1 - \alpha_1')/(\alpha_1 + \alpha_1')$ is in Figs. 4(b) and 4(d). It can be seen that the anisotropy parameter steps over the zero point with the increase of the propagating angle, indicating the existence of an "equivalent point" of two directions at a certain angle, which is consistent with Fig. S3. In addition, this phase diagram also shows that the anisotropy of Rashba effect is nearly independent on laser frequency.

Compared to the isotropic Rashba effect, anisotropic Rashba effect facilitates the generation of spin-polarized electrons [60]. When the GaAs monolayer is doped by electron acceptors, the Fermi level will cross one of the spin channels with the realization of generating spin-polarized electrons

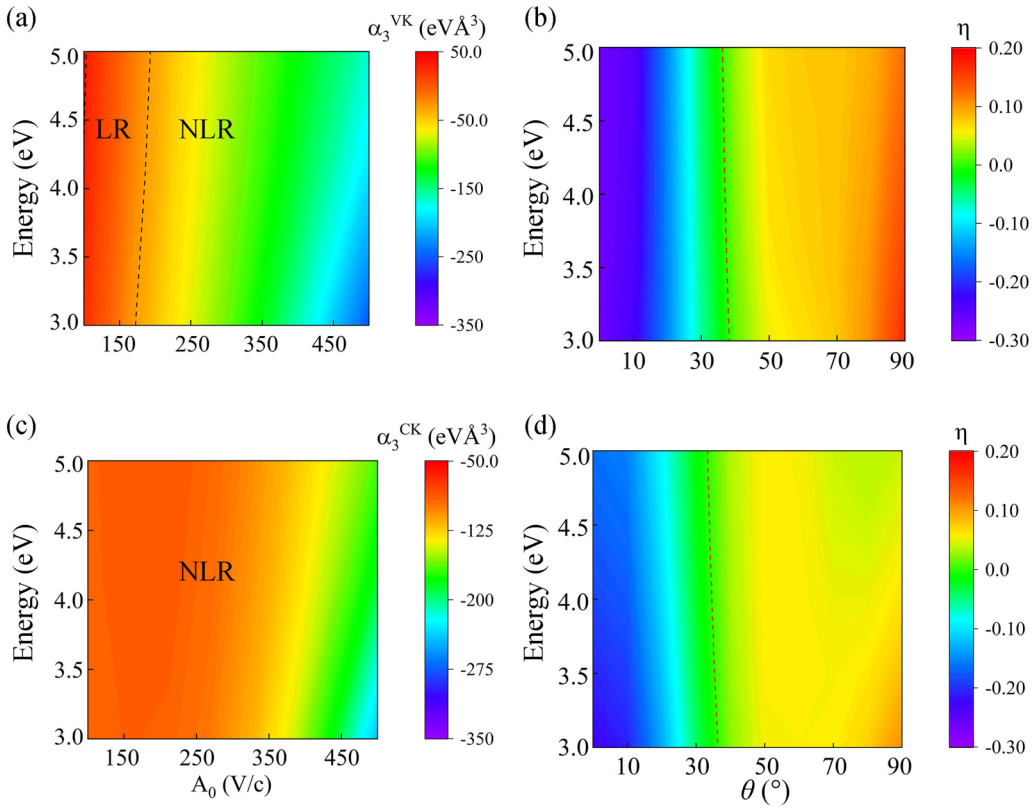

FIG. 4. Phase diagrams of nonlinear coefficient of VB (a), (b) and CB (c), (d) in the (E, A_0) and (E, θ) phase spaces along the Γ-K direction. The phases boundary between linear region (LR) and the nonlinear region (NLR) is indicated by the dashed line. The angle θ is relative to the x axis and the red dashed line is the "equivalent point" of two directions. The amplitude of $A_0 = 500$ V/c for valence band (b) and conduction band (d).

(or spin currents). Moreover, different single spin channels can be selectively obtained since the anisotropic strength of Rashba effect can be tuned by changing the laser propagation direction and laser amplitude. This undoubtedly enriches the flexibility and practicability of the spintronic devices.

Floquet theory provides an experimentally feasible method to regulate electronic states with circularly polarized light, which is not only applicable to topological semiconductors and semimetals, but also to the photonic crystal and cold atom experiments. The previously reported methods of regulating RSS by strain or applied electric field are either causing irreversible damage to the material, or the conditions are too harsh to realize. Our work demonstrates that the periodic laser has a natural modification effect on the electronic structure, which has more abundant controllability in experiment. Moreover, the laser conditions used in the text are readily available under laboratory conditions.

IV. CONCLUSION

In summary, by using first-principles calculations in combination with the Floquet theory, we predict that periodically circularly polarized laser can induce an exotic RSS in the valence and conduction bands of the GaAs monolayer. The laser driven RSS exhibits anisotropic and nonlinear features, which can be described by an effective nonlinear Rashba model involving third-order terms. The anisotropy of nonlinear RSS is mainly determined by the laser propagation direction, providing the possibility of controlling the Rashba anisotropy characteristics. Compared to the Rashba effect via electric field method, the periodic laser can induce an obvious anisotropic Rashba effect, which may allow one to generate spin-polarized electrons and facilitates the flexibility of spintronic devices greatly.

ACKNOWLEDGMENTS

This study is supported by the National Natural Science Foundation of China (No. 12074218), the Special Foundation for Theoretical Physics Research Program of China (No. 11947207), the China Postdoctoral Science Foundation (No. 2020M672039), and the Taishan Scholar Program of Shandong Province.

[1] K. S. Novoselov, A. K. Geim, S. V. Morozov, D. Jiang, Y. Zhang, S. V. Dubonos, I. V. Grigorieva, and A. A. Firsov, Science **306**, 666 (2004).

[2] H. B. Zhang, H. L. Yu, D. H. Bao, S. W. Li, C. X. Wang, and G. W. Yang, Adv. Mater. **24**, 132 (2012).

[3] M. Lang, L. He, F. Xiu, X. X. Yu, J. S. Tang, Y. Wang, X. F. Kou, W. J. Jiang, A. V. Fedorov, and K. L. Wang, ACS Nano **6**, 295 (2012).

[4] I. Žutić, J. Fabian, and S. Das Sarma, Rev. Mod. Phys. **76**, 323 (2004).

[5] W. Yao, D. Xiao, and Q. Niu, Phys. Rev. B **77**, 235406 (2008).
[6] S. Guddala, M. Khatoniar, N. Yama, W. Liu, G. S. Agarwal, and V. M. Menon, Optica **8**, 50 (2021).
[7] H. Şahin, S. Cahangirov, M. Topsakal, E. Bekaroglu, E. Akturk, R. T. Senger, and S. Ciraci, Phys. Rev. B **80**, 155453 (2009).
[8] M. Xu, T. Liang, M. Shi, and H. Chen, Chem. Rev. **113**, 3766 (2013).
[9] J. Wu, Y. Yang, H. Gao, Y. Qi, J. Zhang, Z. Qiao, and W. Ren, AIP Adv. **7**, 035218 (2017).
[10] D. Di Sante, A. Stroppa, P. Barone, M.-H. Whangbo, and S. Picozzi, Phys. Rev. B **91**, 161401(R) (2015).
[11] K. Ueno, T. Shimada, K. Saiki, and A. Koma, Appl. Phys. Lett. **56**, 327 (1990).
[12] Z. Xu, S. Lin, X. Li, S. Zhang, Z. Wu, W. Xu, Y. Lu, and S. Xu, Nano Energy **23**, 89 (2016).
[13] I. Rozahun, T. Bahti, G. He, Y. Ghupur, A. Ablat, and M. Mamat, Appl. Surf. Sci. **441**, 401 (2018).
[14] M. Zhao, X. Chen, L. Li, and X. Zhang, Sci. Rep. **5**, 8441 (2015).
[15] B. P. Bahuguna, L. K. Saini, B. Tiwari, and R. O. Sharma, RSC Adv. **6**, 52920 (2016).
[16] Y. A. Bychkov and E. I. Rashba, J. Phys. C **17**, 6039 (1984).
[17] Y. A. Bychkov and E. I. Rashba, Pis'Ma Zh. Eksp. Teor. Fiz. **39**, 66 (1984) [JETP Lett. **39**, 78 (1984)].
[18] A. Manchon, H. C. Koo, J. Nitta, S. M. Frolov, and R. A. Duine, Nat. Mater. **14**, 871 (2015).
[19] K. Li, X. Xian, J. Wang, and N. Yu, Appl. Surf. Sci. **471**, 18 (2019).
[20] A. Kormányos, V. Zólyomi, N. D. Drummond, and G. Burkard, Phys. Rev. X **4**, 011034 (2014).
[21] S.-J. Gong, C.-G. Duan, Y. Zhu, Z.-Q. Zhu, and J.-H. Chu, Phys. Rev. B **87**, 035403 (2013).
[22] W. Ju, D. Wang, T. Li, H. Wang, Q. Zhou, Y. Xu, H. Li, and S. Gong, J. Phys.: Condens. Matter **32**, 175503 (2020).
[23] P. Titum, N. H. Lindner, M. C. Rechtsman, and G. Refael, Phys. Rev. Lett. **114**, 056801 (2015).
[24] P. Titum, N. H. Lindner, and G. Refael, Phys. Rev. B **96**, 054207 (2017).
[25] N. H. Lindner, G. Refael, and V. Galitski, Nat. Phys. **7**, 490 (2011).
[26] Y. H. Wang, H. Steinberg, P. Jarillo-Herrero, and N. Gedik, Science **342**, 453 (2013).
[27] F. Mahmood, C.-K. Chan, Z. Alpichshev, D. Gardner, Y. Lee, P. A. Lee, and N. Gedik, Nat. Phys. **12**, 306 (2016).
[28] E. J. Sie, J. W. McIver, Y. H. Lee, L. Fu, J. Kong, and N. Gedik, Nat. Mater. **14**, 290 (2015).
[29] J. Kim, X. Hong, C. Jin, S.-F. Shi, C.-Y. S. Chang, M.-H. Chiu, L.-J. Li, and F. Wang, Science **346**, 1205 (2014).
[30] H. Liu, J. T. Sun, C. Cheng, F. Liu, and S. Meng, Phys. Rev. Lett. **120**, 237403 (2018).
[31] U. De Giovannini, H. Hubener, and A. Rubio, Nano Lett. **16**, 7993 (2016).
[32] R. Chen, B. Zhou, and D.-H. Xu, Phys. Rev. B **97**, 155152 (2018).
[33] A. Farrell, A. Arsenault, and T. Pereg-Barnea, Phys. Rev. B **94**, 155304 (2016).
[34] M. A. Sentef, M. Claassen, A. F. Kemper, B. Moritz, T. Oka, J. K. Freericks, and T. P. Devereaux, Nat. Commun. **6**, 7047 (2015).
[35] F. Gesztesy and H. Mitter, J. Phys. A **14**, L79 (1981).
[36] H. Sambe, Phys. Rev. A **7**, 2203 (1973).
[37] J. H. Shirley, Phys. Rev. **138**, B979 (1965).
[38] A. Gomez-Leon and G. Platero, Phys. Rev. Lett. **110**, 200403 (2013).
[39] C.-K. Chan, Y.-T. Oh, J. H. Han, and P. A. Lee, Phys. Rev. B **94**, 121106(R) (2016).
[40] Z. Yan and Z. Wang, Phys. Rev. Lett. **117**, 087402 (2016).
[41] C.-K. Chan, N. H. Lindner, G. Refael, and P. A. Lee, Phys. Rev. B **95**, 041104(R) (2017).
[42] R. W. Bomantara and J. Gong, Phys. Rev. B **94**, 235447 (2016).
[43] R. Wang, B. Wang, R. Shen, L. Sheng, and D. Y. Xing, Europhys. Lett. **105**, 17004 (2014).
[44] H. Hubener, M. A. Sentef, U. De Giovannini, A. F. Kemper, and A. Rubio, Nat. Commun. **8**, 13940 (2017).
[45] K. Taguchi, D.-H. Xu, A. Yamakage, and K. T. Law, Phys. Rev. B **94**, 155206 (2016).
[46] Z. F. Wang, Z. Liu, J. Yang, and F. Liu, Phys. Rev. Lett. **120**, 156406 (2018).
[47] L. Jiang, T. Kitagawa, J. Alicea, A. R. Akhmerov, D. Pekker, G. Refael, J. I. Cirac, E. Demler, M. D. Lukin, and P. Zoller, Phys. Rev. Lett. **106**, 220402 (2011).
[48] Y. Li, A. Kundu, F. Zhong, and B. Seradjeh, Phys. Rev. B **90**, 121401(R) (2014).
[49] M. Benito, A. Gómez-León, V. M. Bastidas, T. Brandes, and G. Platero, Phys. Rev. B **90**, 205127 (2014).
[50] G. Kresse and J. Hafner, Phys. Rev. B: Condens. Matter. **48**, 13115 (1993).
[51] G. Kresse and J. Furthmüller, Phys. Rev. B **54**, 11169 (1996).
[52] J. P. Perdew, K. Burke, and M. Ernzerhof, Phys. Rev. Lett. **77**, 3865 (1996).
[53] G. Kresse and D. Joubert, Phys. Rev. B **59**, 1758 (1999).
[54] J. Liu, W. Hou, L. Sun, X. Ma, X. Feng, T. Nie, and M. Zhao, J. Phys.: Condens. Matter **33**, 145701 (2021).
[55] See Supplemental Material at http://link.aps.org/supplemental/10.1103/PhysRevB.104.085140 for details about the calculation methods and the Floquet analysis, which includes Ref. [56].
[56] U. Herath, P. Tavadze, X. He, E. Bousquet, S. Singh, F. Muñoz, and A. H. Romero, Comput. Phys. Commun. **251**, 107080 (2020).
[57] P. Tsipas, S. Kassavetis, D. Tsoutsou, E. Xenogiannopoulou, E. Golias, S. A. Giamini, C. Grazianetti, D. Chiappe, A. Molle, M. Fanciulli, and A. Dimoulas, Appl. Phys. Lett. **103**, 251605 (2013).
[58] D. C. Camacho-Mojica and F. Lopez-Urias, Sci. Rep. **5**, 17902 (2015).
[59] S. Vajna, E. Simon, A. Szilva, K. Palotas, B. Ujfalussy, and L. Szunyogh, Phys. Rev. B **85**, 075404 (2012).
[60] C. Cheng, J. T. Sun, X. R. Chen, H. X. Fu, and S. Meng, Nanoscale **8**, 17854 (2016).
[61] A. Nuber, M. Higashiguchi, F. Forster, P. Blaha, K. Shimada, and F. Reinert, Phys. Rev. B **78**, 195412 (2008).
[62] E. Simon, A. Szilva, B. Ujfalussy, B. Lazarovits, G. Zarand, and L. Szunyogh, Phys. Rev. B **81**, 235438 (2010).
[63] M. Nagano, A. Kodama, T. Shishidou, and T. Oguchi, J. Phys.: Condens. Matter **21**, 064239 (2009).
[64] S. Lamari, Phys. Rev. B **64**, 245340 (2001).
[65] R. Winkler, Phys. Rev. B **62**, 4245 (2000).
[66] E. A. de Andrada e Silva, G. C. La Rocca, and F. Bassani, Phys. Rev. B **55**, 16293 (1997).
[67] W. Yang and K. Chang, Phys. Rev. B **74**, 193314 (2006).